Article

pubs.acs.org/Biomac

Hemocompatibility of Degrading Polymeric Biomaterials: Degradable Polar Hydrophobic Ionic Polyurethane versus Poly(lactic-*co*-glycolic) Acid

Kathryne S. Brockman,[†,‡] Benjamin F. L. Lai,[§] Jayachandran N. Kizhakkedathu,[§,∥] and J. Paul Santerre*[,†,‡,⊥]

[†]Department of Chemical Engineering and Applied Chemistry, University of Toronto, Toronto, Ontario M5S 3R5, Canada

[‡]Institute of Biomaterials and Biomedical Engineering, Translational Biology and Engineering Program, Ted Rogers Centre for Heart Research, University of Toronto, Toronto, Ontario M5G 1M1, Canada

[§]Department of Pathology and Laboratory Medicine and Centre for Blood Research, University of British Columbia, Vancouver, British Columbia V6T 1Z3, Canada

[∥]Department of Chemistry, University of British Columbia, Vancouver, British Columbia V6T 1Z1, Canada

[⊥]Faculty of Dentistry, University of Toronto, Toronto, Ontario M5G 1G6, Canada

ABSTRACT: The use of degradable polymers in vascular tissue regeneration has sparked the need to characterize polymer biocompatibility during degradation. While tissue compatibility has been frequently addressed, studies on polymer hemocompatibility during degradation are limited. The current study evaluated the differences in hemocompatibility (platelet response, complement activation, and coagulation cascade initiation) between as-made and hydrolyzed poly(lactic-*co*-glycolic) acid (PLGA) and degradable polar hydrophobic ionic polyurethane (D-PHI). Platelet activation decreased (in whole blood) and platelet adhesion decreased (in blood without leukocytes) for degraded versus as-made PLGA. D-PHI showed minimal hemocompatibility changes over degradation. Leukocytes played a major role in mediating platelet activation for samples and controls, as well as influencing platelet-polymer adhesion on the degraded materials. This study demonstrates the importance of assessing the blood compatibility of biomaterials over the course of degradation since the associated changes in surface chemistry and physical state could significantly change biomaterial hemocompatibility.

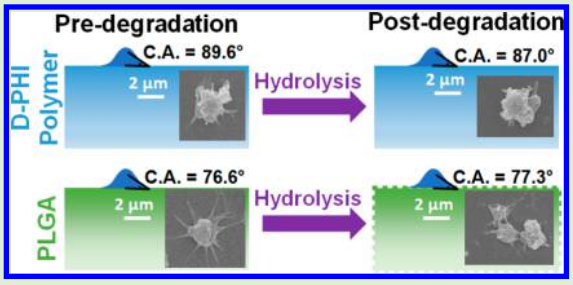

1. INTRODUCTION

Tissue regeneration is a significant focus of current research with regard to biomedical implants. This field is focused on tailoring the degradation of implanted biomaterial scaffolds to optimize the ingrowth and restructuring of tissue. Common synthetic materials being evaluated for this application include poly(lactic-*co*-glycolic acid) (PLGA) and polyurethanes (PUs),[1] both of which can be made into porous scaffolds onto which cells can be seeded and grown into confluent matrices, while the polymer itself degrades into (ideally) noncytotoxic byproducts. Alternatively, polymeric scaffolds are being used as temporary stents in the vasculature with anticipated subsequent regeneration of the endothelium.[2] A focus of research in this field has been to conceive of and synthesize materials with appropriate mechanical properties and biocompatibility for a specified application. Conventionally, biocompatibility studies have primarily focused on testing the properties of the as-made material; however, with the advent of biodegradable materials, there is now a need to address how a material's biocompatibility may change over the course of its resorption as degradation can lead to changes in a polymer's surface chemistry and topography. Recently, this has become a relatively common practice with regard to in vitro and in vivo evaluation of biomaterial cytotoxicity at it relates to tissue cells through studying fibroblasts or endothelial cells.[3−6] However, relatively little attention has been given to blood activation in this regard.

A subset of tissue-engineering polymeric biomaterials are designed to be used in direct contact with blood, such as for vascular grafts and stents. In these cases, it is important to evaluate the hemocompatibility of these materials in order to minimize the possibility of adverse events, such as thrombosis or atherosclerosis leading to blood vessel occlusion. Many studies focus on short-term (typically 1−2 h) analysis to evaluate the effect of the as-made polymers on blood;[7−11] however, these studies are limited in that they only evaluate the initial blood reaction. Clinically, however, numerous blood-contacting devices fail after months to years from late-stage thrombosis or restenosis,[12] which is often believed to be primarily mediated by the biomaterial's thrombogenicity and

Received: March 29, 2017
Revised: June 13, 2017
Published: June 16, 2017

DOI: 10.1021/acs.biomac.7b00456
Biomacromolecules 2017, 18, 2296−2305

compliance mismatch.[13−15] Therefore, questions arise as to why a biomaterial would not have significant problems with thrombogenicity early in its lifetime, but may cause thrombosis later on. A possible reason for this is that changes to the biomaterial, such as material degradation, could result in changes to its surface chemistry and topography, which may affect the material's hemocompatibility. Ideally, this would not be a problem due to cell coverage of the graft protecting the degraded surface from blood contact; however, incomplete cell coverage is often observed early postimplant.[16−18]

Degradation leads to changes in a polymer's surface properties, such as surface chemistry and topography. For example, PLGA, a common biomaterial generally accepted for use in a wide variety of applications, undergoes a bulk degradation mechanism wherein the polymer degrades throughout the entire material, generating lactic and glycolic acids, thus, causing an increase in surface roughness and a weakening of mechanical properties.[19,20] This degradation process occurs largely through hydrolytic cleavage of the ester groups that results in an increase in hydroxyl and carboxylic acid groups.[21,22] It is now commonly acknowledged that a biomaterial's surface properties significantly impact its hemocompatibility, resulting in a substantial body of research on this topic.[2,23−25] This provides further reason to believe that a polymeric biomaterial's degradation (and, therefore, change in surface properties) may impact its hemocompatibility.

To the best of the author's knowledge, the in vitro assessment of blood compatibility of prominent biomaterials as they degrade has not been extensively studied. The present work aims to contribute to the literature by investigating changes in hemocompatibility as a function of biomaterial degradation for an established biomaterial, PLGA (75:25 lactic acid (LA)/glycolic acid (GA)), and a novel degradable PU elastomer, degradable polar hydrophobic ionic polyurethane (D-PHI),[26] which has recently been shown to have good initial blood compatibility.[27] It has been shown that the latter finding was associated with D-PHI's multifunctional surface chemistry (containing ionic, polar, and hydrophobic moieties).[27] The biomaterials underwent hydrolytic degradation using an alkaline medium, and the changes in surface properties were analyzed by contact angle (to evaluate hydrophilicity) and profilometry (to evaluate surface roughness). The degraded and as-made surfaces then underwent hemocompatibility testing by assessing platelet adhesion and activation under flow, complement activation, and coagulation pathway initiation. Where appropriate, these polymers were compared to natural blood and tissue derived biomacromolecule (protein) controls, specifically albumin (low platelet activating) and collagen (high platelet activating).

2. MATERIALS AND METHODS

2.1. Materials. PLGA microspheres (75:25 LA:GA, 75 μm) were purchased from Polysciences Inc. and used as is, polystyrene (PS) particles (600−700 nm) were synthesized as previously described.[28] PS films (Goodfellow, 60 cm wide, 0.05 mm thick) were cut to size (4.5 cm diameter circles) and washed by sonication in Millipore water for 30 min, 70% ethanol for 30 min, and again in Millipore water for 30 min, then allowed to air-dry. PLGA and PS particles were suspended in HEPES (4-(2-hydroxyethyl)-1-piperazineethanesulfonic acid) buffer to a standardized concentration based on estimated surface area (assuming spherical particles and a density of 1 g/cm^3). The surface area was standardized to a 40 g/L solution of D-PHI particles (size = 80.5 ± 28.6 μm dry (scanning electron microscopy (SEM)) and 160 μm wet (Mastersizer 2000, Malvern Instruments)). PS was used as a relative nondegradable standard and positive control for platelet activation.[29]

2.2. D-PHI Synthesis. D-PHI was prepared as described elsewhere.[26] Briefly, a divinyl oligomer (DVO) was synthesized in-house and was mixed with methacrylic acid (MAA; Sigma-Aldrich, ON) and methyl methacrylate (MMA; Sigma-Aldrich, ON) in a molar ratio of 1:5:15 and combined with the initiator benzoyl peroxide (BPO) (0.032 mol per mol of vinyl group). When prepared as smooth films, this mixture was stirred overnight in a closed vessel, then cast on clean glass slides and cured for 24 h at 110 °C under a nitrogen atmosphere. The films were then soaked in Millipore water for 3 h and delaminated from the glass slide using a razor blade. The air-cast side was used for all experiments. For the preparation of particulates, the monomer mixture was stirred with porogens consisting of polyethylene glycol (PEG; Sigma-Aldrich, ON, 10 wt %) and sodium bicarbonate (Sigma-Aldrich, ON, 70 wt %), packed into Teflon molds, and cured for 24 h at 110 °C. The resultant scaffolds were then washed by Soxhlet extraction for 48 h and dried using an ethanol gradient. D-PHI particles were formed by grinding the polymeric sample in a general all-purpose grinder, dedicated specifically to D-PHI so as to eliminate contamination, for 3−5 min and sieving through a 90 μm mesh size sieve to remove large particles (resulting in particles of size 80.5 ± 28.6 μm, estimated using five random SEM regions of interest (ROI)). The particles were suspended in HEPES buffer to a concentration of 40 g/L by sonication (10 min) and vortexing (30 s) immediately prior to use.

2.3. PLGA Film Casting. PLGA beads (Sigma-Aldrich, ON, 75:25 LA:GA, 66−107 kDa) were dissolved in chloroform at 12 wt %, cast onto clean glass slides using a pipet, covered, and allowed to air-dry overnight. The films were then vacuum-dried at room temperature for 3 h and, subsequently, at 50 °C for 3 h. Afterward, the films were incubated in Millipore water for 30 min, and then delaminated from the glass using a razor blade. The air-cast side was used for all experiments.

2.4. Preparation of Collagen and Albumin-Coated PS Films. The collagen coating procedure was modified from an existing protocol.[30] Briefly, Type I rat tail collagen (Sigma-Aldrich, ON, powder) was dissolved in 0.02 N acetic acid at 4 mg/mL in an ice bath. The resulting solution was centrifuged at 4 °C for 1 h at 14000 G, the supernatant was pipetted out and diluted to 0.2 mg/mL in precooled 0.005 N acetic acid. An equal volume of precooled Tris phosphate buffer was added to bring the collagen concentration to 0.1 mg/mL, then the resulting solution (5 mL) was added to a 60 mm Petri dish containing a precleaned PS film (cleaning procedure described in section 2.1). For albumin-coated films, bovine serum albumin (BSA; Sigma-Aldrich, ON) was dissolved in Tyrode's buffer to a concentration of 3 mg/mL, then added (5 mL) to a 60 mm Petri dish containing a precleaned PS film. The films were allowed to incubate overnight at 4 °C prior to cone and plate studies. On the morning of the studies, the films were removed from the protein solutions and gently rinsed with sterile Tyrode's buffer immediately prior to use. These controls were compared to the noncoated PS films.

2.5. Polymer Degradation Studies, Contact Angle, and Profilometry. D-PHI and PLGA films were incubated in 0.1 M potassium hydroxide (KOH) while still adhered to glass slides. The films were removed from solution after 6, 12, 18, 24, and 44 h, rinsed, and allowed to air-dry prior to contact angle and profilometry measurements. Contact angle was measured using a goniometer and surface profile was measured using a surface profilometer (KLA-Tencor P16+). For each reported value, four unique samples were used (for each polymer) and six measurements were taken on each film in different locations. On each spot, the advancing contact angle was measured by slowly increasing the water droplet size using a needle and syringe filled with water, then measuring the contact angle on each side of the droplet. The receding contact angle was measured by a similar procedure where the syringe and needle were used to slowly decrease the water droplet size prior to measurement. Hysteresis was calculated as the difference between the advancing and the receding contact angles. For profilometry, the scan length was 1000 μm, with a scan speed of 20 μm/s and an applied force of 2 mg.

DOI: 10.1021/acs.biomac.7b00456
Biomacromolecules 2017, 18, 2296−2305

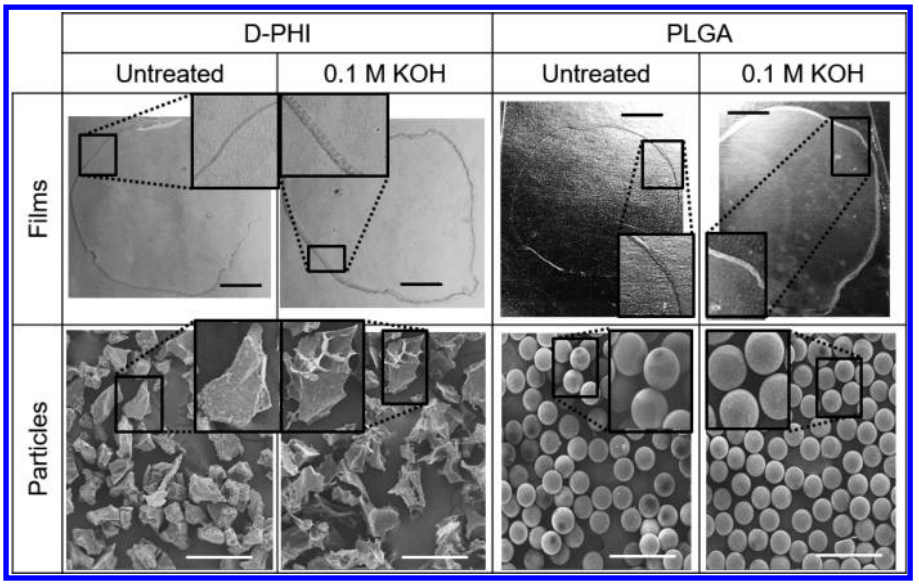

Figure 1. Images of films and particles of D-PHI and PLGA as native materials and after degradation with 0.1 M KOH for 18 h for D-PHI and for 6 h for PLGA. Black scale bars = 1 cm; white scale bars = 200 μm. Zoomed-in (2−2.5×) images show changes over degradation that depict etching for D-PHI (more apparent for films than particles), increased cloudiness and peeling of the edges for PLGA films, but little visible differences for PLGA particles.

The root-mean-square average roughness obtained for each scan (6 per film, four films) was used for analysis.

When preparing samples for blood studies, PLGA films were incubated in 0.1 M KOH for 6 h and D-PHI films were incubated for 18 h since these conditions yielded the greatest change in surface roughness for the respective materials relative to their original state. Optimal treatment conditions used for the final blood compatibility studies were those that produced a detectable chemical change, but were still able to support their physical weight without falling apart while handling. This would provide the ability to compare each degraded polymer against its own original material. Since D-PHI degrades much slower than PLGA, the degradation time needed to be longer for this material in order to achieve a detectable level of degradation in terms of changes to its surface properties. After degradation, the films were thoroughly rinsed with Millipore water and delaminated from their glass support. For particles, incubation conditions were identical to those for the films. Posthydrolysis, the particles were rinsed (by adding Millipore water, vortexing, centrifuging, and removing the supernatant) until the resulting supernatant had a neutral pH. The rinsed particles were freeze-dried and suspended in HEPES buffer as previously described (40 g/L).

2.6. Platelet Adhesion by Cone and Plate Rheometer. Platelet adhesion under shear flow was assessed using fresh, healthy human blood (1.2 mL) drawn into acid citrate dextrose (ACD) collection tubes (University of Toronto ethics approval protocol #22203) and rotated over hydrated films in a cone and plate rheometer[31] at a rate of 150 rpm for 15 min at 37 °C.[32] Films were used for these studies as the design of the system required a flat film for the base over which blood is rotated, and to facilitate the analysis of platelet adhesion and activation on the surface. The films were removed, rinsed with Tyrode's buffer (4×), cut to equal sizes with a 24 mm hole punch, and lysed with 1.8% v/v Triton X-100 in Tyrode's buffer for 1 h at 37 °C. The lactate dehydrogenase (LDH) activity of the supernatant was measured following the protocol of the commercial kit used (CytoTox 96 Non-Radioactive Cytotoxicity Assay by Promega). A calibration curve was generated using serial dilutions of a platelet suspension in Tyrode's buffer. Samples were tested in both human whole blood (WB) and reconstituted human blood, with most of the white blood cells (WBCs) removed (a mix of red blood cells (RBCs) and platelet-rich plasma (PRP)). The mix of RBCs and PRP was obtained using a two-stage centrifugation process wherein WB was first centrifuged at 200*g* for 10 min (with additional 5 min increments as necessary) and the supernatant PRP was removed into a clean falcon tube. The remaining mix of RBCs and WBCs was centrifuged a second time at 1000*g* for 15 min, and the plasma layer and buffy coat were discarded. The resulting RBCs were mixed with the previously obtained PRP to create the RBCs and PRP mix. The samples were tested both with WBCs and without WBCs in order to assess the importance of WBCs in studying platelet−biomaterial interactions. Many studies are conducted with isolated platelets (PRP),[33] and the authors wished to determine the effect of this limitation on the results of platelet-based hemocompatibility experiments.

2.7. Scanning Electron Microscopy (SEM) and Image Analysis. Samples from the cone and plate studies were cut to size and fixed in a 2% gluteraldehyde solution overnight at 4 °C, then dehydrated with increasing concentrations of ethanol (30 min in each 50, 70, 95, and 100%), subjected to critical point drying (CPD), and sputter-coated with 5−10 nm of platinum. For PLGA films, ethanol incubations were shortened to 5 min and CPD was avoided to minimize the loss of sample integrity. Films were rinsed in hexamethyldisilazane (HMDS; Sigma-Aldrich, 99.9%) after removal from 100% ethanol and then incubated in HMDS for 5 min before being allowed to air-dry prior to sputter-coating.[34] Samples were analyzed using a Hitachi S 2500 Scanning Electron Microscope (Hitachi, Mito City, Japan) at an operating voltage of 10 kV (Faculty of Dentistry, University of Toronto). Images were acquired from 10 random ROI on each sample at the same magnification and analyzed using ImageJ software. The image was made binary by setting a threshold value that best separated the surface characteristics (e.g., cells, surface debris) from the background film. Background noise was then removed from the image and the cell sizes were determined using established software commands. Cell sizes were defined by area.

2.8. Activated Partial Thromboplastin Time (APTT) and Dilute Prothrombin Time (DPT) for Blood Coagulation Studies. The APTT assay tests the activation of the intrinsic coagulation pathway, and the dPT assays test the activation of the extrinsic coagulation pathway.[35,36] These assays were conducted as previously described.[37] Blood from healthy, consenting donors was collected into 3.8% sodium citrated tubes with a blood/anticoagulant ratio of 9:1 at the Centre for Blood Research, University of British Columbia (protocol approved by the University of British Columbia's clinical ethics board). Platelet poor plasma (PPP) was prepared by centrifuging citrated whole blood samples at 1200*g* for 20 min. Briefly, PPP (180 μL, prepared by centrifugation) was mixed with particle suspension (20 μL). Particle suspension was used rather than

DOI: 10.1021/acs.biomac.7b00456
Biomacromolecules 2017, 18, 2296−2305

films for these studies due to the significantly higher surface area to volume ratio of particles, which should provide the sensitivity needed to properly assess the material effects on blood elements. For APTT, this solution was mixed with an equal volume of Dade Actin FSL Activated PTT reagent (Siemens), then 100 μL of this mixture was added to a cuvette strip in the STart4 coagulometer (Diagnostica Stago, France) and warmed to 37 °C over 180 s. Finally, 50 μL of 0.025 M $CaCl_2$, warmed to 37 °C, was added to each cuvette, and the time to clot formation was recorded. For dPT, 50 μL of the PPP and particle suspension mixture was added to the STart4 coagulometer to preheat at 37 °C for 60 s, then 100 μL of reagent (thromboplastin-D diluted 100× in 25 mM $CaCl_2$) was added and the time to clot formation measured.

2.9. SC5b-9 (Terminal Complement Complex (TCC)) Complement Activation Studies. Human whole blood was collected (University of Toronto ethics approval protocol #22203) in glass serum tubes (no anticoagulant) and allowed to clot at room temperature for 30 min. The resulting tubes were centrifuged for 20 min at 3000*g* and the serum collected and stored on ice. The human serum was then mixed with particle suspensions in a ratio of 9:1 *v*/*v* and incubated for 1 h at 37 °C with mixing at 20 min intervals. Particle suspensions were used rather than films for these studies due to the significantly higher surface area to volume ratio of particles, which should provide the sensitivity needed to properly assess the material effects on blood elements. A positive control of heat-aggregated immunoglobulin G (IgG) was used (prepared by incubating a 5 mg/mL solution of human IgG in Tris-HCl buffer at 62 °C for 40 min). The resulting solutions were diluted 1:40 with the specimen diluent provided in the MicroVue Complement SC5b-9 Plus EIA kit (Quidel). The remainder of the assay was conducted according to the directions provided for this kit. The resulting concentrations were compared to a five-point calibration curve provided in the kit (0−167 ng/mL, R = 0.99).

2.10. Statistics. Statistical analysis involving *t* tests was conducted using Microsoft Excel in cases where two samples were being compared against each other. One-way ANOVA using IBM SPSS Statistics 21 was used to compare multiple sample groups, with Tukey posthoc used in cases of statistically significant results. Levene's test for the homogeneity of variance was performed for one-way ANOVA and, in cases where the test was not passed, the data set was analyzed by the unequal variance ANOVA equivalent test (Welch) with Dunnett T3 as posthoc analysis. Outliers were removed using the modified Thompson Tau technique. In all cases, α = 0.05.

3. RESULTS

3.1. Polymer Degradation Studies. D-PHI degradation led to visible etching and pitting around the edges of the films and particles (Figure 1). PLGA degradation led to cloudiness in the films but very little visible change to the particles. The degraded PLGA particles were, however, more fragile during handling, despite having been exposed to the alkaline solution for much less time than D-PHI. The contact angle data (Figure 2) shows that both D-PHI and PLGA became more hydrophilic over the course of degradation. Specifically, the advancing and receding contact angles for PLGA significantly decreased over the course of degradation, whereas only the advancing contact angle decreased for D-PHI. The degradation of PLGA caused a significant increase in surface roughness (greater than 10-fold after 6 h of degradation), which then slowly decreased to approximately 5 fold higher than the as-made material and then began to trend upward again (Figure 2B). Conversely, D-PHI showed moderately (although statistically significant) lower surface roughness over the course of degradation (Figure 2B).

3.2. Platelet Adhesion and Activation Analysis. Platelet analysis is one of the main methods used in the literature to evaluate a polymer's hemocompatibility. The ideal method evaluates platelet-biomaterial interaction after exposure to

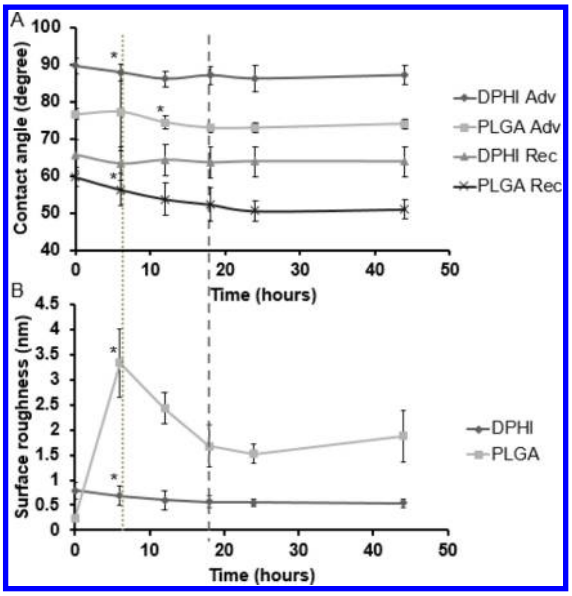

Figure 2. Changes in (A) hydrophilicity by contact angle and (B) surface roughness by profilometry of D-PHI and PLGA films exposed to 0.1 M KOH over 44 h. Data represented as mean ± SE with n = 24 using four distinct samples, and six measurements taken in different locations on each of the samples. The dotted line represents the degradation time chosen for PLGA and the dashed line represents the degradation time chosen for D-PHI for blood studies. * indicates the first time point at which the property is different from that of the same sample at 0 h ($p < 0.05$).

blood under flow, especially with RBCs present, since this most closely replicates in vivo conditions and has been shown to play a significant role in platelet response.[38] The current study used a cone and plate rheometer to replicate blood shear flow over a polymer film surface and studied platelet adhesion and activation to these biomaterials after exposure to WB and blood with the WBCs removed (i.e., a mixture of RBCs and PRP). The adhesion of cells and platelets onto the studied biomaterials is shown in Figure 3 and the level of platelet activation is shown in Figures 4 and 5.

Significantly higher platelet adhesion was seen on the positive controls, collagen and PS, when compared to all other materials in both WB and the mixture of RBCs and PRP (Figure 3A). Once these positive control samples were removed from the analysis, no significant difference was seen between the negative control (albumin) and degraded PLGA exposed to RBCs and PRP, D-PHI, or degraded D-PHI (in either blood solution; Figure 3B). Degraded PLGA exposed to WB and as-made PLGA (in either blood mixture), however, yielded significantly higher platelet adhesion than the albumin-coated substrate. There was no significant difference between platelet adhesion to D-PHI and degraded D-PHI in either blood solution. However, there was significantly less platelet adhesion onto degraded PLGA in RBC and PRP than as-made PLGA in the same blood mixture. Furthermore, there was a significant decrease in platelet adhesion to both of the degraded samples in RBC and PRP when compared to the same degraded films exposed to WB. Finally, there was significantly less platelet adhesion to degraded D-PHI in WB than to degraded PLGA in the same blood solution.

The SEM data qualitatively supported the adhesion data with regard to the number of cells seen on each surface (Figure 4A). Furthermore, there appeared to be very little activation for any

DOI: 10.1021/acs.biomac.7b00456
Biomacromolecules 2017, 18, 2296−2305

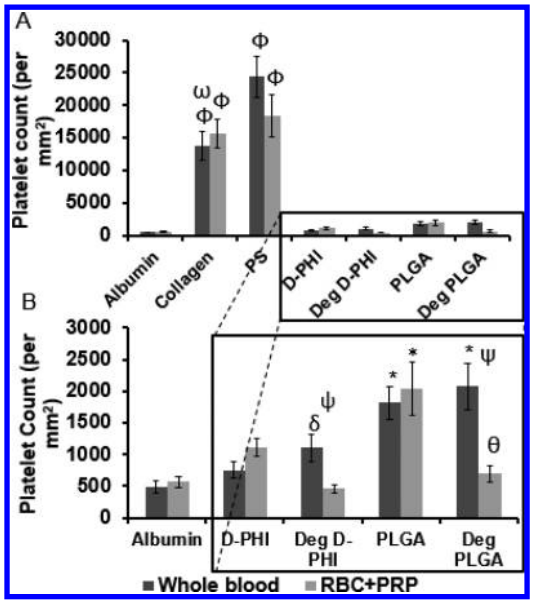

Figure 3. Platelet adhesion to film surfaces after exposure to blood under shear flow by cone and plate rheometer. Data expressed as mean ± SE, n = 11−18, with five different experiments using five different blood donors, three distinct samples per experiment (outliers removed using the modified Thompson Tau technique). Note that "deg" refers to degraded samples. ω $p < 0.05$ different from PS in the same blood solution, ϕ $p < 0.05$ different from all samples except PS and collagen in same blood solution, * $p < 0.05$ different from albumin in same blood solution, δ $p < 0.05$ different from deg PLGA in same blood solution, θ $p < 0.05$ different from PLGA in same blood solution, ψ $p < 0.05$ different between same samples run in different blood solutions.

platelets adhered to albumin, D-PHI, and degraded D-PHI, whereas there was significant pseudopodia formation on collagen, and significant platelet spreading and pseudopodia on PS and PLGA. Degraded PLGA showed a significant amount of smaller surface debris. The SEM results were supported by the data on the percentage of surface area covered by platelets (Figure 4B), which shows that the surface coverage on PS in WB was significantly higher than all other samples except PLGA.

A semiquantitative analysis of platelet activation was achieved by analyzing the particle features on each surface for area and then generating a histogram based on sizes that approximate activation levels (Figure 5). The data was broken into five categories: (1) 1−2 μm^2, mostly debris and some nonactivated platelets; (2) 2−4 μm^2, nonactivated and mildly activated platelets; (3) 4−10 μm^2, activated platelets with significant pseudopodia formation and spreading; (4) 10−80 μm^2, platelet aggregates and other cell types; and (5) 80 μm^2 and greater, large platelet aggregates. Sizes below 1 μm^2 were not considered since this category consisted of a significant amount of noise and confounding forms of debris that cannot be distinguished (e.g., degrading polymer particulate vs platelet microparticles) by SEM alone.

For cells incubated in WB, a good separation was seen for collagen with the largest categories being mildly and heavily activated platelets (categories 2 and 3; Figure 5A). Albumin-coated films and D-PHI had similar distributions with proportionately more mildly activated platelets and other cell types, as compared to heavily activated platelets (Figure 5B). Degraded PLGA had proportionately more particles in category 1. PS and PLGA in WB did not show any particular trend between the different categories; however, these samples showed significantly more surface elements in category 5 (large platelet agglomerates) than the other samples. The analysis of platelet activation for samples tested in a mixture of RBCs and PRP (Figure 5C,D) is difficult to interpret since there was little distinguishable difference between the positive (collagen and PS) and negative (albumin) controls (Figure 5C).

3.3. Blood Coagulation Initiation. Blood coagulation initiation by the polymeric surfaces was measured via APTT for the intrinsic pathway and dPT for the extrinsic pathway, as compared to a normal control of buffer in human PPP. The time to clotting increased for D-PHI and degraded D-PHI when compared HEPES, PS, PLGA, and degraded PLGA when evaluating the intrinsic pathway (Figure 6A). Conversely, time to clot formation decreased slightly for the two D-PHI samples relative to the other materials when evaluating the extrinsic pathway (Figure 6B).

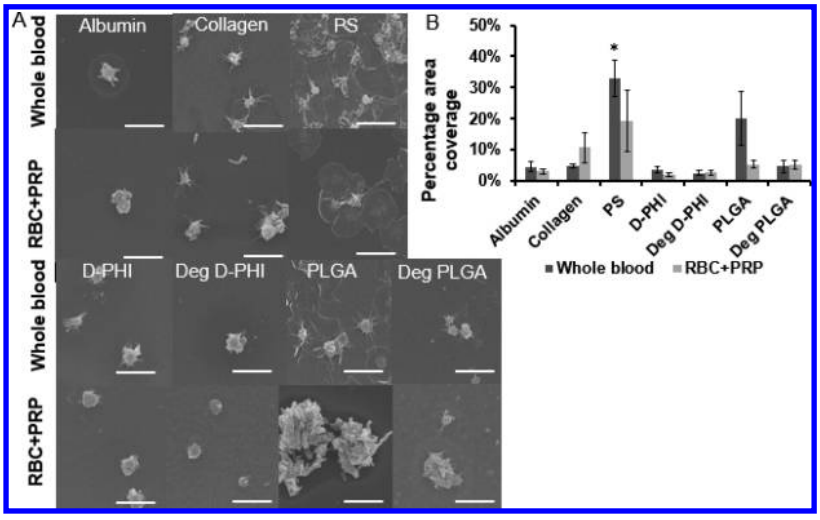

Figure 4. (A) Representative SEM images of platelets on film surfaces and (B) a graph showing the percentage of surface area covered by cells for each film. Data represented as mean ± SE with n = 5 experiments, each using a different blood donor (one sample per experiment, average of 10 images taken from different areas per sample). Scale bar represents 6 μm. * $p < 0.05$ different from all samples except PLGA.

DOI: 10.1021/acs.biomac.7b00456
Biomacromolecules 2017, 18, 2296−2305

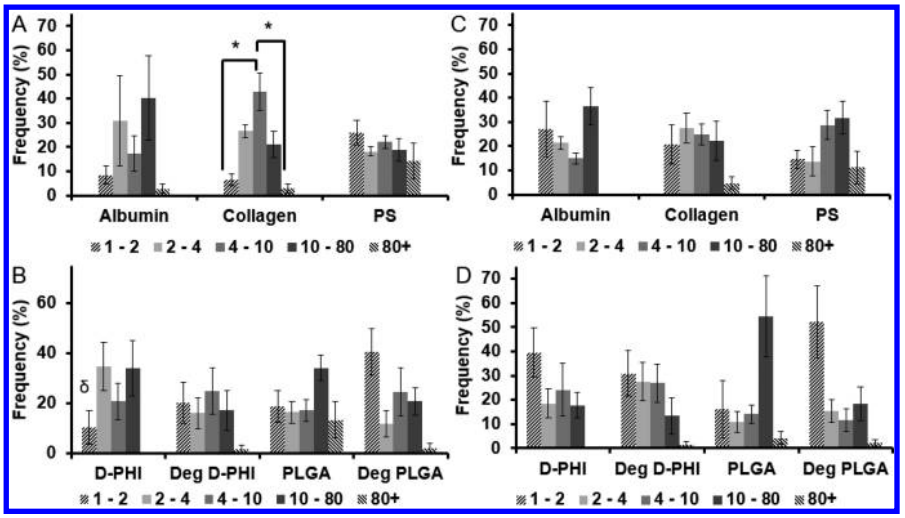

Figure 5. Semiquantitative SEM image analysis data approximating the level of platelet activation on film surfaces from cone and plate by subdividing analyzed cells into five categories based on area. Cell sizes are reported based on frequency of presence for each category. Graphs show results for films incubated in WB (A, B) and a mixture of RBCs and PRP (C, D). Data are split so that controls are shown in (A) and (C) and test samples are shown in (B) and (D). The legends are expressed in units of μm^2. Data expressed as mean ± SE n = 5 experiments, each using a different blood donor (one sample per experiment, average of 10 images, taken from 10 different areas, per sample). * $p < 0.05$ lower than at least one other category for the same sample; δ $p < 0.05$ lower than at least one other sample in the same category.

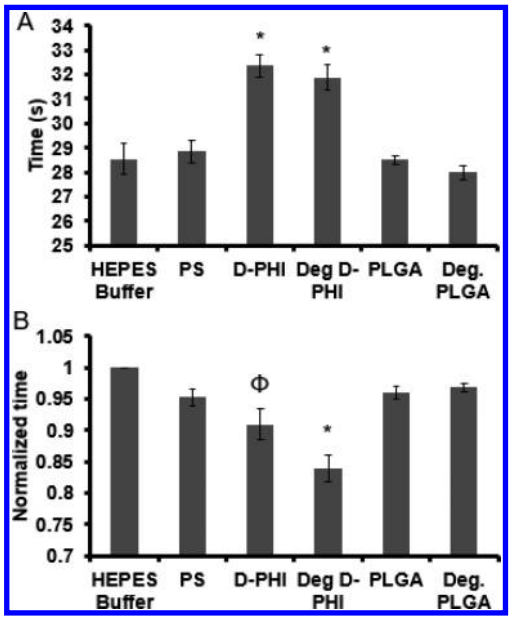

Figure 6. Coagulation cascade activation on biomaterial samples evaluating (A) the intrinsic pathway tested by APTT and (B) the extrinsic pathway tested by dPT for various biomaterials. Data expressed as mean ± SE, n = 9, using three different blood donors, and three distinct samples for each donor. * $p < 0.05$ different from HEPES, PS, PLGA, and degraded PLGA, ϕ $p < 0.05$ different from HEPES.

3.4. Complement Activation. Enzyme-linked immunosorbent assay (ELISA) was performed to evaluate the concentration of the TCC in serum after exposure to different target surfaces. There was a significant increase in the concentration of this complex for PS, D-PHI, and degraded D-PHI when compared to HEPES (Figure 7).

4. DISCUSSION

Biodegradation occurs naturally in vivo through a number of mechanisms, such as hydrolysis, oxidation, or via enzymes.[22]

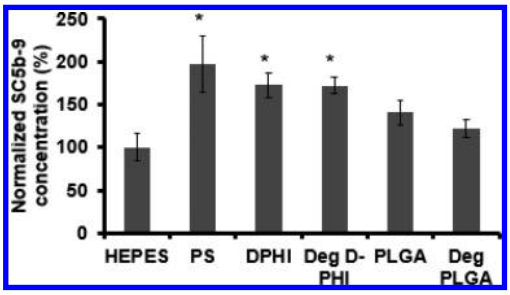

Figure 7. Complement activation assessed by normalized SC5b-9 concentration in serum after exposure to particles of biomaterials. HEPES acts as a normal control and heat-aggregated IgG as a positive control (not shown, 544 ± 121%). Data expressed as mean ± SE, n = 9, with three different blood donors and three distinct samples for each donor. * $p < 0.05$ different from normal control (HEPES).

Attempts to replicate this degradation in vitro is often achieved through the use of buffer, esterases, or proteases.[39,40] However, degradation via this method occurs very slowly for D-PHI.[41] To shorten the hydrolysis time frame and to generate a uniform, clean, and reproducible surface, films were degraded through accelerated hydrolysis using an alkaline solution of 0.1 M KOH and each compared to their own original material. This condition allowed for controlled degradation over the course of hours to days, which led to detectable changes in surface chemistry and topography. Furthermore, this method allowed for easy characterization and maintenance of the polymeric sample's integrity for use in blood compatibility studies.

Visible degradation occurred for both D-PHI and PLGA, as shown by significant changes in both surface chemistry and roughness. PLGA contains ester linkages between each monomer within its backbone. These ester groups are prone to hydrolysis, leading to a subsequent increase in hydroxyl and carboxylic acid groups. As PLGA degrades, it returns to the original monomers of lactic acid and glycolic acid, gradually breaking down the linear polymer. This leads to a bulk degradation mechanism, which explains the rapid increase in surface roughness. D-PHI, however, was deliberately designed

DOI: 10.1021/acs.biomac.7b00456
Biomacromolecules 2017, 18, 2296−2305

to have no aliphatic esters in its central backbone. It is a highly cross-linked polymer that breaks down into lysine, carbon dioxide, hexane diol, and water-soluble oligomeric chains of MMA and MAA.[26] This cross-linking enables D-PHI to follow a surface erosion degradation mechanism, explaining its decrease in surface roughness over the course degradation. There are, however, some ester pendant groups on the cross-linking chains containing MMA that may hydrolyze to carboxylic acid. The latter may help to explain the slightly increased hydrophilicity after degradation. The contact angle values represent a combination of changes in surface chemistry and topography that relate to surface hydrophilicity. There is a slight increase in contact angle (decreased hydrophilicity) for PLGA at 6 h, which is possibly related to the rapid increase in surface roughness; however, the contact angle then decreases to values significantly less than the as-made sample from 12 h onward. The contact angle hysteresis (Figure 8) for PLGA

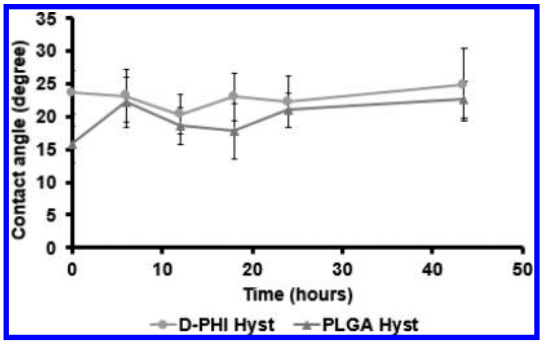

Figure 8. Contact angle hysteresis calculated from the advancing and receding contact angles. Data represented as mean ± SE, with $n = 24$ using four distinct samples and six measurements taken in different locations on each of the polymer films. PLGA hysteresis at 0 h is significantly ($p < 0.05$) different from 12+ h. D-PHI hysteresis at 0 h is not significantly ($p > 0.05$) different from any other time point.

significantly increases from 12 h onward, while it does not significantly change for D-PHI. Hysteresis is typically related to a material's surface energy;[42] therefore, the surface dynamics associated with energy changes appear to be altered for PLGA over the course of degradation, whereas it undergoes no detectable change for D-PHI over the chosen degradation conditions. Overall, there are moderate changes in the surface properties of D-PHI over its degradation, and clear changes in PLGA's surface properties over its degradation.

Relatively good blood compatibility is observed on the as-made degradable polymers (PLGA and D-PHI) since they adhered much fewer platelets than the positive controls (collagen and PS). However, PLGA showed a 4-fold higher amount of platelet adhesion compared to the negative control (albumin) ($p < 0.05$). This sheds new light on this material's propensity to adhere and activate blood elements despite it being widely accepted as a generally biocompatible surface. PLGA's biocompatibility is largely attributed to its ability to degrade into nontoxic byproducts.[43] However, one of PLGA's byproducts, lactic acid, is a known platelet agonist,[44,45] suggesting that blood compatibility for this material could be problematic over time. Alternatively, degraded D-PHI, with its diverse chemistry comprising hydrophilic, hydrophobic, and ionic groups,[26] supports desirable platelet adhesion properties similar to that of albumin.[46] This finding mirrors nondegraded D-PHI, for which it was determined that its inherent mosaic of chemistry mimics protein chemistry in a manner that leads to minor blood activation[27] and favors wound healing.[41]

The authors identified two key observations regarding platelet adhesion to degraded materials (Figure 3). The first was that, in whole blood, there was no significant difference in platelet adhesion between the as-made and degraded materials. The second was that when mixed with blood in the absence of WBCs, degraded polymer films experienced very little platelet adhesion (significantly less than in WB, $p < 0.05$). The latter effect is most interesting since it is not observed for any nondegraded samples (i.e., similar platelet adhesion levels are observed in both WB and blood without WBCs for as-made samples).

Differences in platelet adhesion to as-made versus degraded biomaterials could be related to changes in surface chemistry (polymer surface and/or products), topography, or combinations of these, which in turn both define the surface energy of the materials. Since similar trends are seen in the number of adhered platelet for both D-PHI and PLGA between as-made and degraded films, yet the surface topography changes are opposite, it is unlikely that surface roughness is the cause for these differences. As such, it is more probable that the changes in surface chemistry (evidenced in part by changes in hydrophilicity as noted in the contact angle values) are influencing the manner by which platelets are interacting with degraded samples in the absence of WBCs. The exact mechanism through which WBCs may be mediating this interaction is not completely understood. Several authors have addressed the importance of platelets in leukocyte-biomaterial interactions,[47−53] such as through the expression of P-selectin. Platelets, however, are typically expected to mediate their own adhesion mechanisms through the binding of cell-surface receptors: platelet glycoprotein Ib (GP Ib), platelet glycoprotein IIB/IIIa (GP IIb/IIIa), and P-selectin.[47,51] It has been shown that different adhesion mechanisms exist for leukocytes, depending on the hydrophilicity of the surface to which they are adhering.[54] Taken together, this information may suggest a codependence between platelets and leukocytes with regard to surface adhesion of platelets when specific chemistries are presented (such as a higher proportion of hydroxyl or carboxylic acid groups).[55] The interactions between surface chemistry/topography and blood cells (platelets and leukocytes) is a complicated system. As such, more studies are needed to gain a better understanding of the mechanisms related to the interaction between platelets and leukocytes when mediating blood−biomaterial interactions on degrading polymers with diverse surface properties.

The semiquantitative platelet activation data provided by the SEM analysis yielded more insight into the general level of platelet reactivity with each surface (Figure 5). The key information derived from this graph is provided by category 3 (4−10 μm) type platelets, which is the best indicator of individually separated (as opposed to agglomerated) and highly activated platelets. Categories 4 (10−80 μm) and 5 (80+ μm) are also very indicative of high levels of platelet activation since they include platelet agglomerates, which typically only occur on samples having a very high level of activation. Furthermore, category 4 may also include other cell types or large surface debris from the degradation of the biomaterial, which should be considered as a confounding factor, whereas category 5 shows mostly platelet agglomerates. Category 2 (2−4 μm) provides the best indicator of nonactivated or very mildly activated platelets whereas category 1 (1−2 μm) includes nonactivated

DOI: 10.1021/acs.biomac.7b00456
Biomacromolecules 2017, 18, 2296−2305

platelets but has the confounding factor of encompassing various forms of surface debris, including polymer debris from degrading material. In summary, the discussion will focus on category 2 (mildly activated platelets), category 3 (non-agglomerated, yet activated, platelets), and category 5 (heavily activated and agglomerated platelets).

With this information, a few key points can be drawn from platelet activation studies in WB, Figure 5A,B. The analysis of the control surfaces (Figure 5A) will be completed first as it is instructive in the discussion of the test samples. For the albumin-coated (negative) control, a high proportion of nonactivated/mildly activated platelets (category 2) were seen, as well as other cell types (category 4) when compared to activated platelets (category 3) and platelet agglomerates (category 5). In qualitative observations, the actual number of other cell types (i.e., WBCs and RBCs) on albumin-coated surfaces was similar to that of other samples; however, since there were fewer platelets on albumin, the proportion of adhered cells (RBCs and WBCs) to adhered platelets was higher on albumin than on other samples. While PS had just as much (if not more) platelet adhesion than the positive control (collagen) (Figure 3A), the distribution of platelet activation was quite different (Figures 4 and 5A). Collagen demonstrated a higher proportion of platelets in category 3 (single, highly activated platelets) when compared to the other categories (see Figure 3A, and SEM images to support this conclusion in Figure 4). PS, on the other hand, showed an almost even distribution between all the categories and a relatively high proportion in category 5, as compared to collagen and albumin (Figure 5A). An explanation for this even distribution is that there was an excessive number of platelet agglomerates on the surface, almost to the extent of nearly full surface coverage (see Figure 4A,B), suggesting a highly activating surface that is likely to lead to large thrombus formation and chronic cell activation, including activated WBCs.[56] This was observed in the representative SEM images (Figure 4A) and the percentage surface coverage data (Figure 4B).

The level of platelet activation for the test samples in WB is seen in Figure 5B. D-PHI showed a similar distribution of platelet activation as albumin-coated substrates,[46] suggesting that D-PHI minimally activates platelets (Figure 5A,B). Interestingly, PLGA demonstrated a similar platelet size distribution to PS (Figure 5A,B, and supported by representative SEM images, Figure 4A), indicating a high level of activation for the platelets adhered to these surfaces. This has important implications for blood compatibility if platelets subsequently go on to be activators of leukocytes within the innate immune system, associated with chronic inflammation.[56−58] Providing further support to these observations, it was found that PS and PLGA are the only samples with any significant proportion of adhered surface elements in category 5 (large platelet agglomerates), and that both show a higher level of surface area coverage (Figure 4B). Therefore, while both PLGA and D-PHI show relatively low platelet adhesion (Figure 3A), the level of platelet activation differs between these two samples (Figures 4B and 5B).

Slight differences were observed in the distribution of cell sizes on degraded samples versus their as-made counterparts, although these changes were not statistically significant. Moreover, the level of heavily activated platelets (category 3) on degraded D-PHI is almost identical to that on as-made D-PHI (Figure 5B); however, there appears to be proportionately more cells in category 1 and less in categories 2 and 4 on degraded D-PHI than on the as-made film. This suggests similar levels of platelet activation between as-made and degraded D-PHI (and, therefore, similar hemocompatibility), but potentially more small surface debris on the degraded sample. Note, however, that surface debris is particularly unlikely for D-PHI samples, as the degradation time frame for this material is weeks to months.[41] The increase in small surface debris is more prominent for degraded PLGA versus non-degraded PLGA, where the proportion of particulates in category 1 appears to be much higher than for its nondegraded counterpart (Figure 5B). Furthermore, there is a noticeable decline in categories 4 and 5 (large platelet agglomerates) for degraded PLGA (Figure 5B). This observation is supported by SEM images, which show higher levels of small surface debris (Figure 4A) and lower surface area coverage (Figure 4B) for degraded PLGA when compared to as-made PLGA in WB. This may suggest a potential for less platelet activation (and, therefore, improved hemocompatibility) as PLGA degrades, as indicated by fewer large platelet aggregates and lower surface area coverage. Alternatively, there is a chance that category 1 is predominantly composed of platelet microparticles, which could indicate increased platelet activation.[59] This hypothesis would need further study to evaluate its validity, such as by assessing platelet activation in solution to degraded PLGA particles. Alternatively, the high proportion of category 1 may imply that there is polymer-derived surface debris on the degraded samples; however, the likelihood of substantial degradation debris being generated within the 15 min of the cone and plate studies is minimal. It should be noted that if polymer debris were generated through cone and plate studies, some platelets adhered to and activated on the surface may be removed as well.

It should be pointed out that the activation data appears to be affected by the presence of WBCs for all of the samples (Figure 5C,D) since even the controls expressed abnormal patterns of activation when WBCs were removed (Figure 5C). This is different than the adhesion data, which was only affected by the presence of WBCs for degraded samples (Figure 3B). This observation may indicate the need to include WBCs in any testing done on platelet−biomaterial interactions in order to obtain an accurate biomaterial assessment. The reason that WBCs are required for more physiologically relevant platelet activation is currently not completely understood and is an important area for further study by the field.[47]

Another important consideration is that there is a possibility for changes in platelet activation or platelet consumption in bulk solution (rather than on the biomaterial surface) between as-made and degraded samples. Testing for these effects was not within the scope of the current experiments since the exposure time frames negated the simultaneous influence of degradation products; however, given the differentiated finding for PLGA in this study, this should be considered for future studies in order to gain a more complete picture of the changes in platelet response to as-made versus degraded biomaterials beyond surface-adhered cells.

The assessment of the protein pathways (Figures 6 and 7) yielded no major differences between the degraded and as-made samples in either materials' case. The only differences observed were a slight decrease in clotting time for the extrinsic pathway of the coagulation cascade for degraded D-PHI versus as-made, and a slight decrease in complement activation for degraded PLGA versus as-made. However, these changes can be viewed as negligible since they are not statistically significant

DOI: 10.1021/acs.biomac.7b00456
Biomacromolecules 2017, 18, 2296−2305

between the respective degraded and nondegraded samples. Since tests for changes in protein-related activation pathways look specifically for changes in bulk solution, it is possible that differences would be more prominent if soluble degradation byproducts were present rather than just the degraded particle surfaces.[44,45,60] These studies were completed with particles of polymers rather than films (which were used in the platelet studies) since particles allowed for easier suspension in solution and higher surface area to volume ratios, which are expected to amplify any observed effect. Despite this, no significant changes were seen, which suggests that plasma proteins play less of a role than cellular blood components in biomaterial surface-initiated thrombosis between degraded and nondegraded surfaces since cellular blood components showed a significant effect even with a small biomaterial surface area (e.g. cone and plate studies).

5. CONCLUSIONS

Overall, there are some important differences in platelet adhesion and activation on the surfaces of biomaterials when comparing their before and after degradation states, yet no significant differences in bulk coagulation and complement protein activation. Specifically, no significant changes were seen in the hemocompatibility of D-PHI before and after degradation in any of the studies, which is consistent with the minimal changes in surface chemistry and topography observed over the course of degradation. Degraded PLGA, on the other hand, showed a slight decrease in platelet adhesion (only when WBCs are not present) and an apparent decrease in surface-adhered platelet activation (in WB) when compared to the as-made control; however, as discussed, platelet lysis could by playing a role. The observed differences may be related to changes in polymer surface chemistry or topography, such as the increase in hydrophilic character, increase in surface roughness, or change in surface energy seen for degraded PLGA. However, it should be noted that, despite being statistically significant, the contact angle change for PLGA is relatively minor. Therefore, it is possible that the differences in platelet behavior could be due to factors other than hydrophilicity that occurred during degradation and have not been considered here. It should also be considered that there may be limitations in the degradation mechanism in this study since it focuses solely on hydrolysis, whereas it may be possible for D-PHI and PLGA to also undergo an oxidative degradation mechanism when exposed to macrophages,[61] which could cause different surface chemistry changes.

An important conclusion from this study is that WBCs play a central role in mediating platelet adhesion to degraded polymeric surfaces and platelet activation on all polymer samples (pre- and postdegradation). This suggests the need for further research to completely elucidate the mechanism through which WBCs affect platelet adhesion and activation. Specifically, it would be beneficial to evaluate how specific polymeric surface chemistries play a role in platelet adhesion and activation on biomaterials, as well as the importance of WBCs in mediating these mechanisms.

To the best of the authors' knowledge, this is the first study evaluating hemocompatibility changes in biomaterials before and after degradation using a well-controlled in vitro environment and studying the coagulation, PRP, and WB models together. The design was such that degradation could be easily characterized and controlled, which was necessary to ensure sufficient sample integrity and reproducibility for the experiments.

AUTHOR INFORMATION

Corresponding Author

*E-mail: paul.santerre@utoronto.ca. Phone: 416-946-8158. Fax: 416-979-4760.

ORCID

J. Paul Santerre: 0000-0003-3373-6463

Author Contributions

The manuscript was written through contributions of all authors. All authors have given approval to the final version of the manuscript.

Funding

Natural Sciences and Engineering Research Council (NSERC) # Syn 430828, NSERC Canada Graduate Scholarship-Masters (CGSM), NSERC Discovery Grant, Career Investigator Scholar Award from the Michael Smith Foundation for Health Research, Queen Elizabeth II Graduate Scholarship in Science and Technology, and NSERC Collaborative Research and Training Experience Program (CREATE).

Notes

The authors declare no competing financial interest.

ACKNOWLEDGMENTS

The study was supported by the Natural Sciences and Engineering Research Council (NSERC) # Syn 430828, NSERC Canada Graduate Scholarship-Masters (CGSM), Queen Elizabeth II Graduate Scholarship in Science and Technology, and NSERC Collaborative Research and Training Experience Program (CREATE). Thank you to Kai Yu for synthesizing the PS particles. J.N.K. holds a Career Investigator Scholar award from the Michael Smith Foundation for Health Research (MSFHR). J.N.K. also acknowledges NSERC Discovery Grant support.

REFERENCES

(1) Nair, L. S.; Laurencin, C. T. *Prog. Polym. Sci.* **2007**, *32* (8−9), 762−798.

(2) Jung, F.; Wischke, C.; Lendlein, A. *MRS Bull.* **2010**, *35* (08), 607−613.

(3) van Minnen, B.; Stegenga, B.; van Leeuwen, M. B. M.; van Kooten, T. G.; Bos, R. R. M. *J. Biomed. Mater. Res., Part A* **2006**, *76* (2), 377−385.

(4) Yeganegi, M.; Kandel, R. a; Santerre, J. P. *Acta Biomater.* **2010**, *6* (10), 3847−3855.

(5) Guelcher, S. A. *Tissue Eng., Part B* **2008**, *14* (1), 3−17.

(6) Deshayes, S.; Kasko, A. M. *J. Polym. Sci., Part A: Polym. Chem.* **2013**, *51* (17), 3531−3566.

(7) DeFife, K. M.; Grako, K.; Cruz-Aranda, G.; Price, S.; Chantung, R.; Macpherson, K.; Khoshabeh, R.; Gopalan, S.; Turnell, W. G. *J. Biomater. Sci., Polym. Ed.* **2009**, *20* (11), 1495−1511.

(8) Renò, F.; Traina, V.; Cannas, M. *J. Biomater. Sci., Polym. Ed.* **2007**, *18* (6), 785−797.

(9) Koh, L. B.; Rodriguez, I.; Zhou, J. *J. Biomed. Mater. Res., Part A* **2008**, *86* (2), 394−401.

(10) Nguyen, K. T.; Su, S.-H.; Sheng, A.; Wawro, D.; Schwade, N. D.; Brouse, C. F.; Greilich, P. E.; Tang, L.; Eberhart, R. C. *Biomaterials* **2003**, *24* (28), 5191−5201.

(11) Wolfe, P. S.; Madurantakam, P.; Garg, K.; Sell, S. a; Beckman, M. J.; Bowlin, G. L. *J. Biomed. Mater. Res., Part A* **2010**, *92* (4), 1321−1328.

(12) Schoen, F. J.; Padera, R. F., Jr. *Biomaterials Science: An Introduction to Materials in Medicine*; Elsevier, 2011; pp 771−784.

DOI: 10.1021/acs.biomac.7b00456
Biomacromolecules 2017, 18, 2296−2305

(13) Kapadia, M. R.; Popowich, D. A.; Kibbe, M. R. *Circulation* **2008**, *117* (14), 1873−1882.
(14) Owens, C. D.; Ho, K. J.; Conte, M. S. *Vasc. Med.* **2008**, *13* (1), 63−74.
(15) Seifalian, A. M.; Tiwari, A.; Hamilton, G.; Salacinski, H. J. *Artif. Organs* **2002**, *26* (4), 307−320.
(16) Ravi, S.; Chaikof, E. *Regener. Med.* **2010**, *5* (1), 1−21.
(17) Foxall, T. L.; Auger, K. R.; Callow, A. D.; Libby, P. *J. Surg. Res.* **1986**, *41* (2), 158−172.
(18) Enomoto, S.; Sumi, M.; Kajimoto, K.; Nakazawa, Y.; Takahashi, R.; Takabayashi, C.; Asakura, T.; Sata, M. *J. Vasc. Surg.* **2010**, *51* (1), 155−164.
(19) Shirazi, R. N.; Aldabbagh, F.; Erxleben, A.; Rochev, Y.; McHugh, P. *Acta Biomater.* **2014**, *10* (11), 4695−4703.
(20) Engineer, C.; Parikh, J.; Raval, A. *Trends Biomater. Artif. Organs* **2011**, *25* (2), 79−85.
(21) Nair, L. S.; Laurencin, C. T. *Adv. Biochem Engin/Biotechnol* **2006**, *102* (October 2005), 47−90.
(22) Treiser, M.; Abramson, S.; Langer, R.; Kohn, J. *Degradable and Resorbable Biomaterials*; Elsevier, 2013.
(23) Toufik, J.; Carreno, M. P.; Jozefowicz, M.; Labarre, D. *Biomaterials* **1995**, *16* (13), 993−1002.
(24) Jukarainen, H. J.; Clarson, S. J.; Seppälä, J. V.; Retzinger, G. S.; Ruohonen, J. K. *Silicon* **2011**, *4*, 1−8.
(25) Koh, L. B.; Rodriguez, I.; Venkatraman, S. S. *Biomaterials* **2010**, *31* (7), 1533−1545.
(26) Sharifpoor, S.; Labow, R. S.; Santerre, J. P. *Biomacromolecules* **2009**, *10* (10), 2729−2739.
(27) Brockman, K. S.; Kizhakkedathu, J. N.; Santerre, J. P. *Acta Biomater.* **2017**, *48*, 368−377.
(28) Kizhakkedathu, J. N.; Norris-jones, R.; Brooks, D. E. *Macromolecules* **2004**, *37* (3), 734−743.
(29) Shenkman, B.; Savion, N.; Dardik, R.; Tamarin, I.; Varon, D. *Thromb. Res.* **2000**, *99*, 353−361.
(30) Rajan, N.; Habermehl, J.; Coté, M.-F.; Doillon, C. J.; Mantovani, D. *Nat. Protoc.* **2006**, *1* (6), 2753−2758.
(31) Skarja, G. a; Kinlough-Rathbone, R. L.; Perry, D. W.; Rubens, F. D.; Brash, J. L. *J. Biomed. Mater. Res.* **1997**, *34* (4), 427−438.
(32) Massa, T. M.; Yang, M. L.; Ho, J. Y. C.; Brash, J. L.; Santerre, J. P. *Biomaterials* **2005**, *26* (35), 7367−7376.
(33) Jung, F.; Braune, S.; Lendlein, a. *Clin. Hemorheol. Microcirc.* **2013**, *53* (1−2), 97−115.
(34) McBane, J. E.; Battiston, K. G.; Wadhwani, A.; Sharifpoor, S.; Labow, R. S.; Santerre, J. P. *Biomaterials* **2011**, *32* (14), 3584−3595.
(35) Kainthan, R. K.; Janzen, J.; Levin, E.; Devine, D. V.; Brooks, D. E. *Biomacromolecules* **2006**, *7* (3), 703−709.
(36) Kainthan, R. K.; Gnanamani, M.; Ganguli, M.; Ghosh, T.; Brooks, D. E.; Maiti, S.; Kizhakkedathu, J. N. *Biomaterials* **2006**, *27* (31), 5377−5390.
(37) Ahmed, M.; Lai, B. F. L.; Kizhakkedathu, J. N.; Narain, R. *Bioconjugate Chem.* **2012**, *23* (5), 1050.
(38) Horbett, T. A. *Evaluation of Blood−Materials Interactions*; Elsevier, 2013.
(39) Lu, L.; Garcia, C. a; Mikos, a G. *J. Biomed. Mater. Res.* **1999**, *46* (2), 236−244.
(40) Tang, Y. W.; Labow, R. S.; Santerre, J. P. *J. Biomed. Mater. Res.* **2001**, *57* (4), 597−611.
(41) McBane, J. E.; Sharifpoor, S.; Cai, K.; Labow, R. S.; Santerre, J. P. *Biomaterials* **2011**, *32* (26), 6034−6044.
(42) Gao, L.; Mccarthy, T. J. *Langmuir* **2006**, *22* (14), 6234−6237.
(43) Yoon, S. J.; Kim, S. H.; Ha, H. J.; Ko, Y. K.; So, J. W.; Kim, M. S.; Yang, Y. Il; Khang, G.; Rhee, J. M.; Lee, H. B. *Tissue Eng., Part A* **2008**, *14* (4), 539−547.
(44) Babensee, J. E.; Paranjpe, A. *J. Biomed. Mater. Res., Part A* **2005**, *74A* (4), 503−510.
(45) Kilkson, H.; Holme, S.; Murphy, S. *Blood* **1984**, *64* (2), 406−414.
(46) Munro, M. S.; Quattrone, A. J.; Ellsworth, S. R.; Kulkarni, P.; Eberhart, R. C. *Trans. Am. Soc. Artif. Int. Organs* **1981**, *27* (1), 499−503.
(47) Gorbet, M. B.; Sefton, M. V. *Biomaterials* **2004**, *25* (26), 5681−5703.
(48) Rinder, H. M.; Bonan, J. L.; Rinder, C. S.; Ault, K. a; Smith, B. R. *Blood* **1991**, *78* (7), 1730−1737.
(49) Mickelson, J. K.; Lakkis, N. M.; Villarreal-Levy, G.; Hughes, B. J.; Smith, C. W. *J. Am. Coll. Cardiol.* **1996**, *28* (2), 345−353.
(50) Mitchell, M. J.; Lin, K. S.; King, M. R. *Biophys. J.* **2014**, *106* (10), 2243−2253.
(51) Hu, H.; Varon, D.; Hjemdahl, P.; Savion, N.; Schulman, S.; Li, N. *Thromb. Haemostasis* **2003**, *No. 5930*, 679−687.
(52) Spectre, G.; Zhu, L.; Ersoy, M.; Hjemdahl, P.; Savion, N.; Varon, D.; Li, N. *Thromb. Haemostasis* **2012**, *108* (2), 328−337.
(53) Asimakopoulos, G.; Taylor, K. M. *Ann. Thorac. Surg.* **1998**, *66* (6), 2135−2144.
(54) Eriksson, C.; Nygren, H. *J. Lab. Clin. Med.* **2001**, *137* (4), 296−302.
(55) Thevenot, P.; Hu, W.; Tang, L. *Curr. Top. Med. Chem.* **2008**, *8* (4), 270−280.
(56) Gawaz, M.; Langer, H.; May, A. E. *J. Clin. Invest.* **2005**, *115* (12), 3378−3384.
(57) Ekdahl, K. N.; Lambris, J. D.; Elwing, H.; Ricklin, D.; Nilsson, P. H.; Teramura, Y.; Nicholls, I. A.; Nilsson, B. *Adv. Drug Delivery Rev.* **2011**, *63* (12), 1042−1050.
(58) Anderson, J. M.; Rodriguez, A.; Chang, D. T. *Semin. Immunol.* **2008**, *20* (2), 86−100.
(59) Diamant, M.; Tushuizen, M. E.; Sturk, A.; Nieuwland, R. *Eur. J. Clin. Invest.* **2004**, *34* (6), 392−401.
(60) Middleton, J. C.; Tipton, A. J. *Biomaterials* **2000**, *21* (23), 2335−2346.
(61) Mcbane, J. E.; Santerre, J. P.; Labow, R. S. *J. Biomed. Mater. Res., Part A* **2007**, *82* (4), 984−994.

DOI: 10.1021/acs.biomac.7b00456
Biomacromolecules 2017, 18, 2296−2305